THE JOURNAL OF PHYSICAL CHEMISTRY C

Article

Cite This: J. Phys. Chem. C 2018, 122, 26756−26763

pubs.acs.org/JPCC

Multiply-Binding Polymeric Imidazole Ligands: Influence of Molecular Weight and Monomer Sequence on Colloidal Quantum Dot Stability

John H. Dunlap, Abigail F. Loszko,[†] Raeven A. Flake, Yucheng Huang, Brian C. Benicewicz, and Andrew B. Greytak*

Department of Chemistry and Biochemistry, University of South Carolina, Columbia, South Carolina 29208, United States

Supporting Information

ABSTRACT: This study addresses the colloidal stability of polymer-coated core/shell CdSe/$Cd_xZn_{1-x}S$ quantum dots (QDs) in the presence of L-glutathione (GSH) under neutral conditions by means of photoluminescence (PL) and absorption spectroscopy. A reversible addition−fragmentation chain-transfer-mediated synthesis was employed to produce co-polymer ligands with different molecular weights in block and random sequences. Poly(ethylene glycol) sidechains were incorporated on a methacrylate backbone for solubility in phosphate-buffered saline. Imidazole-bearing histamine sidechains were installed postsynthetically to facilitate binding to the QD surface. Introduction of L-glutathione, an endogenous monothiol, to aqueous solutions of the polymer-coated QDs led to an increase in PL quantum yield, indicating an interaction between the QD and glutathione. The PL change was greatly diminished for block co-polymers versus random co-polymers of similar molecular weight and composition. Additionally, higher ligand populations were found upon initial purification of block co-polymer-coated QDs versus the random co-polymers. We demonstrate that glutathione does not significantly displace the polymer ligands from the QD surface, suggesting that PL changes are driven primarily through ligand association. The block co-polymers are more resistant to glutathione association, and indeed stronger binders, than the randomly ordered co-polymers, with higher-molecular-weight contributing to improved stability in both cases. To the best of our knowledge, this is the first study to directly compare the relative stability of block and random polymeric imidazole ligands and should aid in developing more stable ligand-exchanged QDs for bioimaging and biosensing, especially for in vivo and intracellular applications.

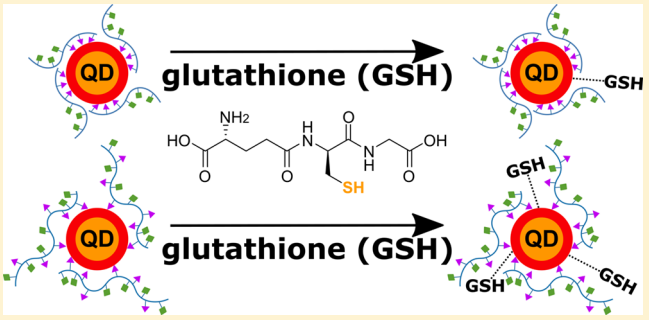

1. INTRODUCTION

Colloidal semiconductor quantum dots (QDs) are attractive fluorophores for bioimaging and biosensing applications owing to their photostability, size-tunable emission, and high molar extinction coefficients. Core/shell QDs (e.g., CdSe/CdS, CdSe/$Cd_xZn_{1-x}S$, etc.) are widely employed for bioimaging experiments, as they better maintain their high quantum yields (QYs) when transferred into aqueous media. Yet, QDs with shells of several monolayers' thickness remain sensitive to surface conditions. As-synthesized QDs possess surfaces passivated by hydrophobic ligands, which inhibit dispersion in polar solvents, but are vital to maintaining control during nucleation and growth. Postsynthetic modifications with hydrophilic molecules must therefore be employed to satisfy general requirements for biological applications. These include colloidal stability in water (over time and at a range of pH values), high QYs, low acute toxicity, and low nonspecific binding.[1]

A variety of strategies have been developed for transferring QDs into aqueous media, which rely on using surfactants or amphiphilic polymers to encapsulate the QD and native ligands, or ligand-exchange reactions to fully replace native ligands on the surface. Amphiphilic polymers effectively encapsulate natively capped QDs via micelle-like structures, but these strategies often result in large hydrodynamic radii and limit their use as fluorescent probes.[2,3] However, smaller sizes may be retained by utilizing ligand-exchange reactions to install hydrophilic surfaces with anionic, cationic, steric, or zwitterionic stabilization. Small molecule thiols, such as cysteine, readily displace native ligands and lead to water-soluble QDs that can exhibit high QYs in some cases, particularly with ZnS-based shells in the case of CdSe QDs.[4] Multiple groups have demonstrated that QD stability may be improved by incorporating bidentate binding schemes, such as poly(ethylene glycol) (PEG)-modified dihydrolipoic acid ligands, on core/shell QDs.[5,6] These QDs exhibited low nonspecific binding and improved stability over a wide pH range. However, they do not provide sufficient protection of

Received: September 13, 2018
Revised: October 30, 2018
Published: November 1, 2018

Downloaded via UNIV OF SOUTH CAROLINA COLUMBIA on February 20, 2019 at 16:06:13 (UTC).
See https://pubs.acs.org/sharingguidelines for options on how to legitimately share published articles.

© 2018 American Chemical Society

DOI: 10.1021/acs.jpcc.8b08984
J. Phys. Chem. C 2018, 122, 26756−26763

the QD surface, being prone to oxidation, poor long-term stability, and low QY in the case of thinner or less confining shells.[7−10]

Further improvements in stability can be achieved with polymeric ligands containing multiple anchor groups that can bind to the QD surface; such polymers can also incorporate hydrophilic moieties for solubility and functional groups for further modification.[11−13] This approach is exemplified by synthetic polymers bearing imidazole sidechains that mimic the polyhistidine motif that has previously been used to anchor polypeptides to QD surfaces. More recently, Mattoussi's group has demonstrated multidentate polymer-QD systems involving both histamine and lipoic acid functionalities to yield stable and compact QDs.[14] This multiply-binding strategy addressed concerns regarding the weak surface−imidazole bond and thiol oxidation.[15] The imidazole group possesses an affinity to under-coordinated metal sites on the QD surface, is resistant to oxidation, and has been shown to maintain high quantum yields and facilitate stable QD colloids in aqueous media.[11,16−19]

Despite numerous reports on multiply-binding co-polymer ligands, there has been relatively little exploration of differences resulting from varying monomer sequences within such polymers. A common method for forming multiply binding or multidentate co-polymers relies on the ring opening of poly(isobutylene-*alt*-maleic anhydride) (PIMA) by nucleophilic addition of amine-modified monomers. The maleic anhydride readily reacts with primary amines, enabling formation of modified co-polymers without the need for coupling agents.[20−22] This technique has been used to form a variety of amphiphilic co-polymers for passivating nanoparticles, with imidazole and/or thiol anchors, zwitterion motifs, and reactive groups for further functionalization, but does not offer control of the sequence of residues.[14,20−24] Another polymerization method, reversible addition−fragmentation chain transfer (RAFT), involves the free-radical polymerization of monomers through utilization of a chain-transfer agent. As a living or controlled polymerization technique, it is possible to construct block co-polymers by sequentially introducing monomers in the desired order with low polydispersities and good control over the molecular weight.[25] Work by Lequeux and co-workers described the use of multidentate zwitterion/vinylimidazole block co-polymers, which demonstrated the efficacy of imidazole-binding block co-polymers to yield stable QD samples.[26,27] Alternatively, if all monomers are introduced initially, then polymer sequence is determined statistically according to relative reactivity ratios of the monomers, resulting in disordered sequences. This method has been the approach in most published examples to date, including our own work.[17] Bawendi and co-workers pursued a strategy in which various monomers synthesized with PEG chains, imidazole groups, and derivatizable groups for further functionalization were combined into a monomer mixture of differing ratios initiated by RAFT polymerization.[11] However, the effects of sequence and length have yet to be directly compared in this or other classes of polymeric imidazole ligands.

A key characteristic for QD surface coatings to be used in imaging live cells or organisms, especially in intracellular applications, is to resist interference or ligand displacement by endogenous compounds. In particular, the intracellular stability of polymer-capped QDs is of great concern because endogenous thiol molecules, especially glutathione (GSH) and cysteine, are present at high concentrations to maintain redox homeostasis, and could potentially displace polymers relying on imidazole as the anchoring group.

Zhu et al. used laser desorption/ionization mass spectrometry to quantify changes in dithiolate ligand monolayers on CdSe/ZnS QDs upon exposure to intracellular GSH, demonstrating that monolayer stability in HeLa cells can be compromised.[7] This provided evidence that naturally occurring thiols are capable of displacing surface ligands at biologically relevant concentrations (which can reach up to 10 mM), leading to possible aggregation, leaching of toxic metal ions, and decrease in function.[7] Understanding how endogenous thiols interact with polymer-capped QDs, and the influence of polymer structure, sequence, and length on this interaction, is essential for designing QDs appropriate for biomedical applications.

Our group has developed a family of methacrylate-based polymeric imidazole ligands (MA-PILs) synthesized by RAFT. The methacrylate backbone reduced the potential for premature reaction during synthesis compared to acrylate monomers. The polymer-capped QDs (MA-PIL-QDs) were stable and exhibited negligible nonspecific binding and cytotoxicity to human endothelial cells over a range of polymer chain lengths.[18] Ternary co-polymers with methoxy- and amine-terminated PEG sidechains enabled selective labeling of targets on cell surfaces via copper-free click chemistry and were also used to demonstrate association of MA-PILs to CdS nanowires through the use of a covalently linked fluorescent dye tracer.[19,28]

In the present study, we directly examine the stability of MA-PIL-capped CdSe/$Cd_xZn_{1-x}S$ core/shell QDs toward small thiol molecule competition, using glutathione at biologically relevant concentrations under neutral conditions in phosphate-buffered saline (PBS, pH 7.3−7.5). The core/shell QDs were prepared by selective ion layer addition and reaction (SILAR) and purified by gel permeation chromatography (GPC) in toluene prior to ligand exchange to install the MA-PILs, according to previously described methods.[17,29] Four MA-PILs were designed with a combination of PEG and imidazole sidechains using RAFT-mediated co-polymerization to define disordered (random) or block co-polymers (Scheme 1). In each case, two different average polymer lengths were prepared, incorporating poly(ethylene glycol)methacrylate (PEGMA-475) and *N*-methacrylol succinimide (NMS)

Scheme 1. MA-PIL Ligands and L-Glutathione Competitor

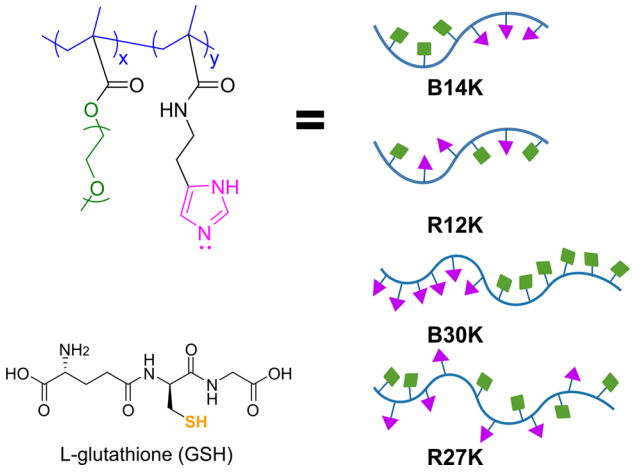

DOI: 10.1021/acs.jpcc.8b08984
J. Phys. Chem. C 2018, 122, 26756−26763

Table 1. Summary of Block and Random Co-polymer Composition, Molecular Weight, Dispersity ($Đ$), and Degree of Polymerization (DP)

		M_n			DP[b]	
co-polymer	polymer ID	GPC	NMR	dispersity ($Đ$[a])	PEGMA	NMS
poly(PEGMA-*b*-NMS)	**B14K**	12 000	13 700	1.10	21	18
poly(PEGMA-*b*-NMS)	**B30K**	17 100	29 600	1.13	44	45
poly(PEGMA-*co*-NMS)	**R12K**	13 500	12 400	1.29	18	19
poly(PEGMA-*co*-NMS)	**R27K**	24 500	27 300	1.39	40	43

[a]Measured by GPC. [b]Calculated by monomer conversion from ^{1}H NMR.

monomers. Imidazole anchoring groups were installed post-polymerization by a quantitative reaction of the succinimidyl esters with histamine. Block co-polymers were synthesized with average molecular weights of 14 and 30 kDa, herein referred to as **B14K** and **B30K**. Random co-polymers were synthesized with average molecular weights of 12 and 27 kDa, herein referred to as **R12K** and **R27K**. The stability of the ligand-exchanged QDs to GSH exposure was tested in two ways. First, the photoluminescence of the MA-PIL-QDs was monitored to detect surface interactions with GSH since the QY is known to be sensitive to ligand-exchange or association processes, and because QY is relevant to the imaging and sensing applications of QDs. Secondly, the ligand population on the QD surface was directly measured by ultraviolet−visible (UV−vis) absorption spectroscopy and used to quantify the ligand-to-QD ratio after removing unbound molecules via centrifugal dialysis filtration. The results to follow suggest that block co-polymers exhibit superior stability and diminished interference from small molecules, whereas in both cases the larger co-polymers appear to be more robust toward such molecules. This demonstrates the influence of molecular weight and monomer sequence on the stability of colloidal polymer-capped QDs with respect to glutathione, a representative competing ligand. To the best of our knowledge, this is the first direct comparison of polymer binding strength and resistance to small molecule competition as a function of monomer sequence. The findings that block co-polymers exhibit superior stability and diminished interference from small thiol molecules may be applicable to other classes of polymeric ligands and provides new insights into the development of stable, robust polymeric ligand coatings for in vivo and in vitro bioimaging and sensing applications.

2. EXPERIMENTAL METHODS

2.1. Materials and Characterization. A detailed description of all materials and methods used for the synthesis and characterization of poly(PEGMA-*b*-imidazole) ligands and CdSe/$Cd_xZn_{1-x}S$ quantum dots is provided in the Supporting Information.

2.2. Photoluminescence Spectroscopy. The MA-PIL-QDs were first dialyzed in deionized water using centrifugal spin concentrators (regenerated cellulose membrane) to remove excess free polymer and diluted in PBS buffer (pH 7.4). The purified sample was then brought to 20 mL in N_2-sparged PBS. For each PL titration trial, a 2.5 mL aliquot of the diluted QD sample was transferred to a N_2-filled septum-capped quartz cuvette with a stir bar. The cuvette was placed in a holder atop a stir plate and covered to prevent ambient light exposure. A syringe was filled with L-glutathione (44.52 mM in PBS) and secured onto a syringe pump, configured to inject 100 μL GSH every 15 min via glass capillary until a total concentration of ∼8 mM GSH was reached. Emission spectra were collected under constant 365 nm excitation. Prior to the first GSH injection, the spectrum was monitored for 15 min to account for the QD PL response. A control experiment was performed using N_2-sparged PBS in place of GSH to account for any influence of dilution on the PL response.

2.3. Quantification of Polymer Ligands on the QD Surface. A digestion assay coupled with UV−vis absorption spectroscopy was used to quantify the amount of bound polymer on the QD surface after exposure to specific environmental conditions. A 1 nmol aliquot of the MA-PIL-QDs was passed through a 0.2 μm poly(ether sulfone) syringe filter and dialyzed in PBS buffer (pH 7.4). For each dialysis process, the sample was initially concentrated (5 min/5000 rpm), followed by five cycles of dialysis in PBS (5−10 min/5000 rpm) to achieve consistently low retention volumes (∼100 μL). The retained QDs were diluted in PBS for analysis and divided into three portions. Portion A was immediately digested in ∼2 mL HCl (3 M) by stirring in the dark for 1 h, after which the absorption spectrum was recorded. Portion B was diluted in 2 mL GSH (2 mM in PBS) and sparged with N_2 for 10 min followed by stirring in the dark for 1 h. Portion B was then dialyzed into PBS to remove free GSH, and the retentate diluted in PBS for absorption measurements. Finally, the sample was digested in ∼2 mL HCl with stirring in the dark for 1 h, followed by another absorption measurement. A control sample (portion C) was designed to account for potential dilution effects that may occur with the GSH-treated sample. Portion C underwent the same treatment as portion B, using clean PBS buffer in place of the GSH solution.

3. RESULTS AND DISCUSSION

3.1. Synthesis of MA-PIL Ligands. A previously reported RAFT-mediated synthesis was used to prepare the poly(PEGMA-*co*-imidazole) ligands with tailored molecular weights and low polydispersities (Table 1).[17] The reactivity ratios of the NMS (r_1 = 0.91) and PEGMA (r_2 = 0.69) monomers were determined by the Kelen−Tudos method.[17] As their reactivities are relatively similar, the monomers could be co-polymerized, attaching to the methacrylate backbone in such a manner that they become randomly distributed along the polymer chain. For the block co-polymers on the other hand, poly(PEGMA-*b*-imidazole) was synthesized by sequentially polymerizing the monomers along the methacrylate backbone. In the case of the block co-polymers, the PEGMA was prepared first to form PEG monomers close to the R-group, quenched, and then the NMS monomers were polymerized. Since the succinimidyl group of NMS readily reacts with primary amines, histamine was introduced after successful removal of the RAFT agent to install imidazole anchors; the co-polymers were then isolated by dialysis. A

DOI: 10.1021/acs.jpcc.8b08984
J. Phys. Chem. C 2018, 122, 26756−26763

schematic representation of the final MA-PIL ligand structures is provided in Scheme 1.

3.2. Preparation of Core/Shell QDs with MA-PIL Co-polymer Ligands. The CdSe/$Cd_xZn_{1-x}S$ QDs were synthesized via the previously reported SILAR method, natively capped with oleate and phosphonate ligands.[29] A four monolayer $Cd_xZn_{1-x}S$ shell was coated onto the CdSe cores. The shell growth was monitored by absorption and emission spectroscopy, with the QDs emitting at 572.5 nm. Prior to ligand exchange, the QDs were purified by GPC in toluene with a polystyrene size-exclusion medium to remove small molecule impurities and weakly bound ligands. Our group has previously shown the efficacy of GPC as a preparative technique for stable nanocrystal colloids with consistently low ligand-to-QD ratios, providing a surface which facilitates efficient ligand exchanges.[29,30] In the discussion to follow, the polymer-capped QDs will be referred to by the bound polymer type as follows: **B14K-QD**, **B30K-QD**, **R12K-QD**, and **R27K-QD**.

To facilitate aqueous dispersion, the native hydrophobic ligands on the QD surface were exchanged with the MA-PIL ligands by solution-phase ligand exchange. The QDs, fully dried under vacuum after GPC purification, were dispersed in chloroform in the presence of excess ligand and stirred under ambient conditions. After stirring in chloroform for 45 min, methanol was added to separate the polymer-capped QDs from the organic ligands. After an additional 20 min, the QDs were flocculated by the addition of a 1:6 ethanol/hexane mixture, centrifuged, and the MA-PIL-QDs isolated as a solid before dispersing in PBS (pH 7.4). Figure 1 shows

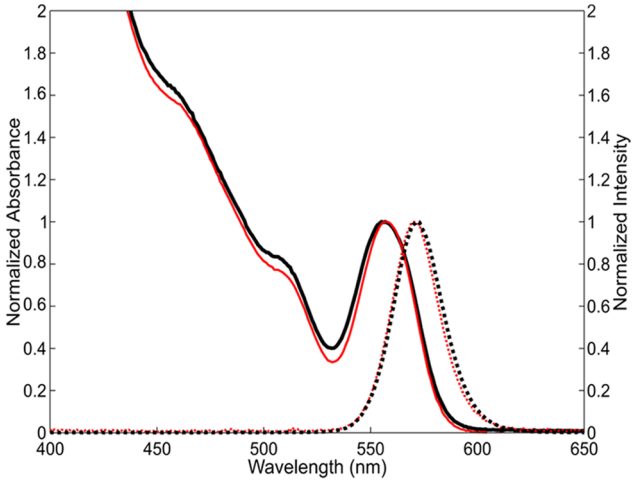

Figure 1. Normalized absorption and PL emission spectra of CdSe/$Cd_xZn_{1-x}S$ QDs. Absorption (solid lines: heavy/black, after GPC in toluene; thin/red, **B14K-QD** after ligand exchange in PBS) is normalized at 557 nm. Emission of respective samples (dashed lines) is normalized at maximum intensity.

representative absorption and emission spectra of a QD sample before and after ligand exchange. The QDs show minimal changes in the primary exciton peak line shape, with only a slight red shift in the peak wavelength following ligand exchange. Likewise, the emission spectra before and after ligand exchange are quite similar, with a small blue shift following ligand exchange. This demonstrates that the ligand-exchange method has little impact on the optoelectronic properties of the QDs. Prior to the glutathione exposure studies below, the aqueous MA-PIL-QDs were subjected to multiple cycles of dialysis using ultrafiltration membranes to remove excess free polymer, then diluted in PBS.

3.3. Photoluminescence Response to Glutathione. Except in the case of very thick and electronically isolating shells, the QY of colloidal QDs can be very sensitive to ligand association and dissociation processes at the surface.[31,32] Thus, we utilized PL spectroscopy to characterize changes in PL in response to GSH at biologically relevant concentrations for each MA-PIL-QD combination. Specifically, to evaluate whether an interaction occurs between GSH and the MA-PIL-QDs, a titration experiment was designed in which the PL response was monitored continuously while GSH was introduced stepwise in a series of aliquots. Any change in QY caused by introduction of GSH could then be detected and used to compare the response of samples with random and block co-polymer ordering.

The MA-PIL-QDs were placed in an air-tight cuvette with stirring, and a complete spectrum was collected every 10 s under 365 nm excitation. The spectra were integrated after baseline subtraction to give an intensity value that could be plotted as a function of time. With each GSH injection, the QD concentration decreased by a known amount due to the increase in total volume. Accordingly, the intensity values following injections are scaled up based on the ratio between the current and final volume following each addition of GSH. Examination of the emission spectra over the course of the experiment showed no significant change in emission line shape. Under these conditions, changes in scaled intensity are directly proportional to changes in PLQY.

Several controls were put in place to isolate the response to GSH exposure. Due to the constant light exposure necessary for successive PL response studies, the drift in the PLQY of the MA-PIL-QDs in PBS was monitored in the dark (Figure S2). In these measurements, the QDs were only exposed to light long enough to record a full spectrum and stirred for 5 min between subsequent measurements. All samples show an increase in PL over time, with block co-polymer-capped QDs demonstrating less drift than their random co-polymer-capped QD analogs. A control titration with N_2-sparged PBS was also conducted to account for dilution effects on the PLQY (Figure S3). The sample was stirred in PBS under constant light exposure, wherein 0.1 mL of PBS was titrated into the cuvette via syringe pump every 15 min, and the PL monitored over time.

Figure 2 shows the experimental design for the GSH-response measurements and the corresponding PL traces for each MA-PIL-QD. In brief, the MA-PIL-QDs (nominally 62.6 nM in N_2-sparged PBS) were sealed in a N_2-filled cuvette (to limit oxidation of the GSH) and stirred in the dark under ambient conditions. For the first 15 min of each trial, the QD PL was monitored prior to addition of GSH to test their behavior under constant light exposure. The GSH was introduced via incremental titration over time and the PL intensity continuously monitored for changes in peak position and intensity (full experimental details are located in the Supporting Information). The total GSH concentration was kept below 8 mM to avoid significant changes in the pH. Each GSH injection was administered swiftly every 900 s to allow sufficient time for an equilibrium to be reached, so that any rapid response to subsequent increases in [GSH] would be evident.

DOI: 10.1021/acs.jpcc.8b08984
J. Phys. Chem. C 2018, 122, 26756−26763

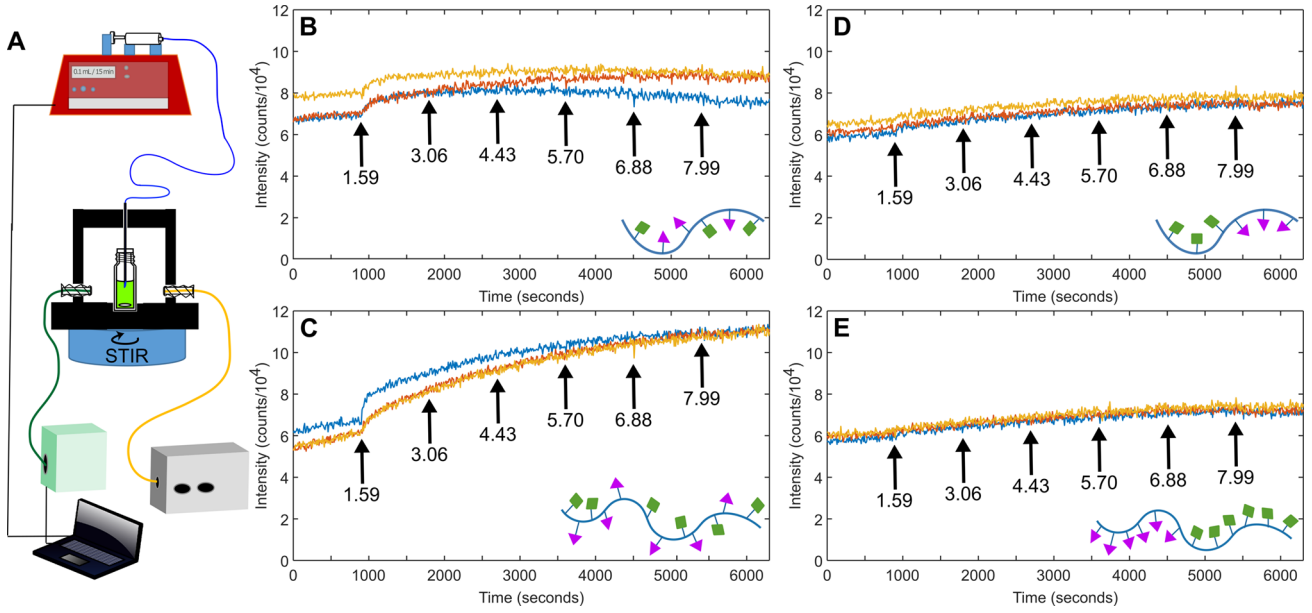

Figure 2. Integrated PL intensities in response to glutathione titration. (A) Experimental design for PL measurements. (B–E) Integrated PL response to GSH for **R12K-QD**, **R27K-QD**, **B14K-QD**, and **B30K-QD**, respectively in PBS. Arrows indicate injection times and the total [GSH] in millimolar following each injection. Measurements were repeated in triplicate, with individual trials indicated by different colors (red, orange, and blue). All intensity values were corrected for dilution of the QD concentration.

Scheme 2. Digestion Assay To Measure MA-PIL/QD Ratio and Detect Displacement by GSH

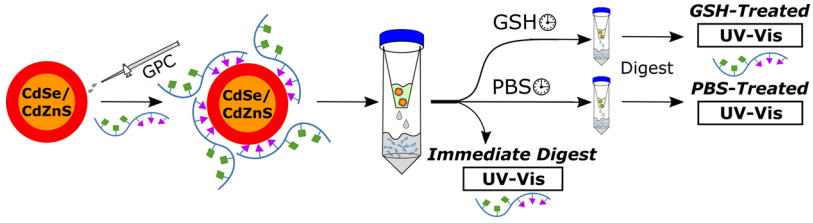

The data presented in Figure 2 provides a qualitative comparison between the influence of monomer sequence and molecular weight in response to glutathione. At times prior to the first GSH injection, the QDs show a slow drift toward higher PL. However, upon initial addition of GSH, a small increase in PLQY on a timescale of several minutes is observed in all cases. The random co-polymer-capped QDs show a substantially larger increase in PL with respect to their block co-polymer-capped QD analogs. In the PBS control titrations (Figure S3), no change is discernable at the injection times. This suggests that block co-polymer MA-PILs are more resistant to interactions with GSH. We observe that the extent of change in PL at each concentration point and the equilibration time, after which the intensity no longer changes rapidly, is most pronounced at the first injection, when the GSH concentration goes from 0 to 1.59 mM, suggesting an effective association constant (K_a) $\geq 10^3$ M^{-1} for the underlying process. Though PL clearly indicates that an interaction occurs and that it is diminished for the block co-polymer-capped QDs, PL response alone is not indicative of the nature of this reaction. To gain further information regarding this interaction, we turn to absorption spectroscopy.

3.4. Quantification of Polymer Ligand Populations. In a ligand association process, the binding of an incoming molecule (i.e., GSH) does not alter the population of the native ligands on the QD surface. In a ligand exchange, however, the native ligands are displaced from the surface by a competing molecule and liberated as free ligand in solution. To distinguish between these processes, we quantified the ratios of polymer-to-QD after introduction of GSH and subsequent repurification to remove unbound polymer using UV–vis absorption spectroscopy. In comparison to other quantification methods such as ^{1}H NMR, UV–vis is well suited for studying ligand interactions, as it does not require high analyte concentrations or deuterated solvents. The histamine imidazole group served as a spectroscopic handle owing to its strong UV absorption at 213 nm, whereas the QDs absorb in the visible range at 557 nm. However, the QDs absorb strongly at short wavelengths and therefore the amounts must be measured separately, with the ligand measurement performed after completely digesting the QDs in acidic solution and dilution to known volume.

Scheme 2 outlines the experimental approach for the digestion assay. Hydrochloric acid was found to be an effective means of degrading the QDs without destroying the polymer, allowing the polymer absorption to be resolved after digestion. Following ligand exchange to prepare the MA-PIL-QDs, 1 nmol of QDs was subjected to multiple cycles of centrifugal dialysis in PBS to remove excess free polymer and weakly bound polymer. We define this as the initially purified sample, nominally containing only QDs with bound polymer ligands. Each sample was divided into three portions of equal volume. Portion A was immediately analyzed to determine the initial ligand content. Because the largest increase in PL intensity

DOI: 10.1021/acs.jpcc.8b08984
J. Phys. Chem. C 2018, 122, 26756–26763

occurred at low concentrations of GSH, we used 2 mM GSH in PBS for the digestion assay. Portion B was exposed to the GSH under N_2, stirred for 1 h, then dialyzed in PBS to remove excess GSH before analysis. Portion C was used as a control sample for GSH treatment and underwent an identical treatment to portion B, but using clean PBS in place of GSH. The QD concentration before repurification in portion B was approximately 125 nM for each MA-PIL-QD sample. A representative trial for GSH-treated **B14K-QD** is provided in Figure 3.

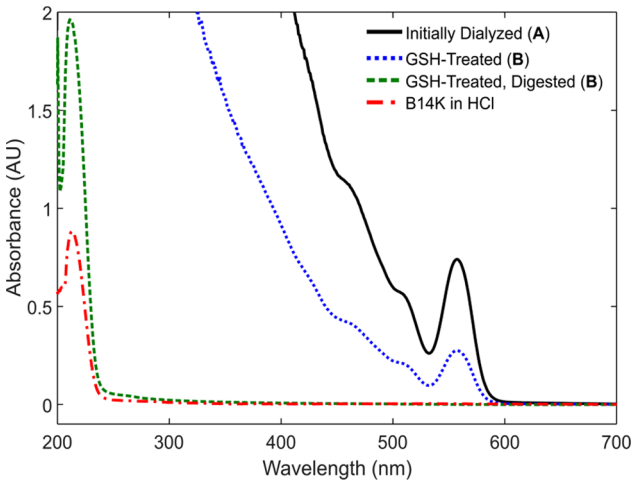

Figure 3. Representative absorption spectra for **B14K-QD** after dialysis, GSH treatment, and digestion. A reference spectrum of **B14K** in HCl is also shown.

The absorption of the dialyzed, GSH-treated sample was used to measure the total QD concentration. After the addition of HCl, the sample no longer exhibits any visible absorption feature at 557 nm, indicating the efficacy of the digestion. The polymer is readily identifiable in acid, with no significant changes in line shape or peak wavelength. The QD and imidazole absorption data for each sample were used to assign the molar quantities of QDs and surface-bound MA-PILs by comparing the visible and ultraviolet peak heights, respectively, to those of reference samples of known concentration.

Figure 4 compares the raw spectra and scaled reference curves for **B14K-QD** before (visible) and after (UV) digestion. Since no significant changes in QD absorption and emission were detected after ligand exchange, the QD concentrations were determined based on the extinction coefficient measured at 350 nm in toluene, 2.24×10^6 M^{-1} cm^{-1}.

The results from the digestion assay and concentration fitting are summarized by the average polymer/QD mole ratios for each MA-PIL-QD sample in Figure 5. When comparing the block and random co-polymer ligands, the block ligand mole ratios were consistently higher, indicating a greater residual ligand population following ligand exchange and centrifugal dialysis in PBS. To understand the role of glutathione and the stability of the different polymer coatings, the GSH- and PBS-treated experiments must be compared. These samples undergo further dialysis in PBS after treatment, thus if GSH displaces the polymer, a lower polymer content should be present after digestion (with respect to the PBS control). In other words, ligand exchange by GSH would be indicated by a lower polymer/QD ratio in portion B than portion C, whereas indistinguishable polymer/QD ratios between these portions

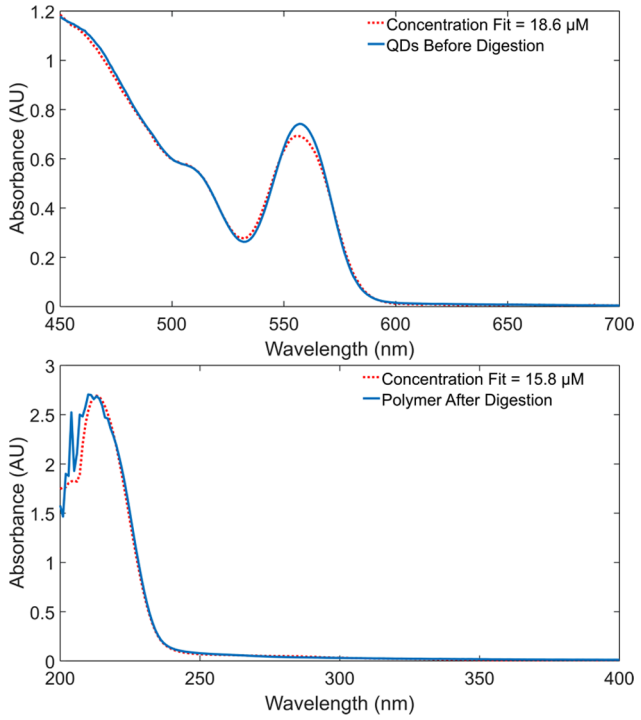

Figure 4. Representative concentration fits for **B14K-QD** (portion A) via absorption spectroscopy showing QDs before digestion (top) and polymer after digestion (bottom) absorption. The sample and fitting spectra are shown by the solid and dashed lines, respectively.

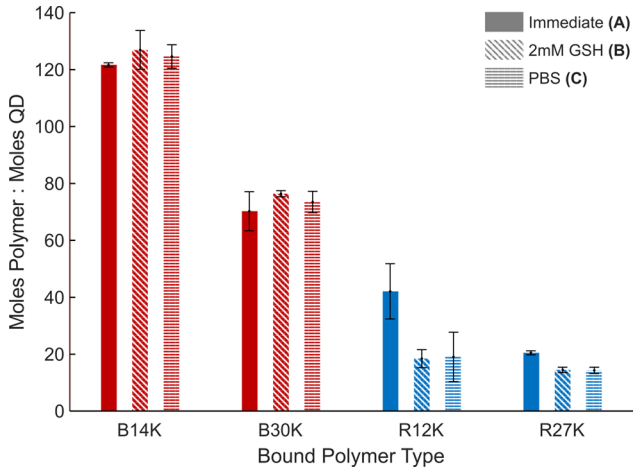

Figure 5. Average MA-PIL/QD mole ratios for the three portions of each sample. All assays were repeated in triplicate and error bars indicate 1 standard deviation.

would be indicative of association. Considering only the effect of monomer sequence, the block co-polymer ligands were present at higher mole ratios after GSH treatment (vs the random polymers), suggesting that block co-polymer MA-PILs have a higher affinity for the QD surface. Since there is no substantial difference between the GSH- and PBS-treated mole ratios in any of the MA-PIL formulations in this study, we conclude that GSH does not drive displacement of the polymer ligands. Yet, at low concentrations and the same timescale, significant PL changes were observed. This indicates that such PL changes are likely driven by GSH association to vacant binding sites on the QD surface. The random co-polymers exhibit lower ligand-to-QD ratios following initial

DOI: 10.1021/acs.jpcc.8b08984
J. Phys. Chem. C 2018, 122, 26756−26763

dialysis and continue to lose ligand upon dilution and subsequent dialysis, which could contribute to a higher number of accessible surface sites to which GSH can bind. The larger polymers, **B30K** and **R27K**, appear to yield QDs that are more robust and resistant to interactions with GSH than the shorter polymers of similar sequence. This is indicated by better retention of the **R27K** versus **R12K** upon repeated dilution and purification in Figure 5, and by the diminished PL response of **B30K** versus **B14K** in Figure 2.

4. CONCLUSIONS

We prepared stable CdSe/$Cd_xZn_{1-x}S$ core/shell QD colloids with methacrylate-based polymeric imidazole ligands. By controlling the order of monomer addition, we synthesized block- and randomly ordered co-polymers consisting of a methacrylate backbone, PEG groups for dispersion in PBS, and imidazole anchors for binding to the QD surface. The application of RAFT-mediated synthesis facilitated the preparation of co-polymers with a high degree of molecular weight tunability. The QDs were purified by GPC to remove small molecule impurities and weakly bound organic ligands prior to ligand exchange with the polymers. We directly probed the stability of the MA-PIL-QDs toward glutathione at biologically relevant concentrations (up to 8 mM) in PBS (pH 7.4) and studied whether GSH binds with the QD through association to vacant sites or by displacing the polymeric ligands through exchange.

PL spectroscopy revealed that upon initial titration of GSH, the random co-polymer-capped QDs exhibited a substantially greater increase in PL in contrast to the block co-polymer-capped QDs. This suggested that the block MA-PILs were more resistant to glutathione interactions. In regard to this increase in PL, we note that ligand exchange with thiols has been found previously to lead to lower QY compared to PILs. The small increases here could be a result of the rigorous dialysis protocol used to strip unbound MA-PIL ligands prior to the experiment or to the use of air-free conditions to limit thiol oxidation.

By means of a digestion assay and absorption spectroscopy, we quantified the mole ratios of polymer-to-QD. The QD and polymer concentrations were determined by fitting their visible and UV absorption with reference spectra before and after digestion in acid, respectively. The consistently higher ratios of block ligands to QDs suggest that a higher ligand population is present after ligand exchange and dialysis. When exposed to GSH, the random co-polymer populations were consistently smaller, suggesting that they have a lower affinity for the QD surface. In all cases, when comparing the GSH-exposed samples to control experiments, we find that the differences in polymer-to-QD mole ratios are not substantial, suggesting that GSH does not displace the co-polymer ligands. In the case of the differing molecular weights, we note that the higher-molecular-weight co-polymers (**B30K** and **R27K**) are more robust and resistant to GSH at low concentrations (2 mM). On the basis of the PL and absorption data, we conclude that GSH association occurs regardless of polymer size or monomer sequence, albeit to a significantly higher degree for the random co-polymers. Therefore, block co-polymer imidazole ligands are more effective at stabilizing CdSe/$Cd_xZn_{1-x}S$ QDs in the presence of endogenous small thiol molecules in aqueous buffer at biologically relevant concentrations.

The superior stability and diminished interference of block co-polymers to biogenic thiols highlight the importance of monomer sequence on colloidal QD stability for live cell and intracellular applications. We believe that this work serves as a stepping stone for developing more effective multiply binding co-polymer coatings for bioimaging and biosensing. Future studies into imidazole-bearing block co-polymers could focus on analyzing their stability in vivo, under a range of pH conditions, and the influence of other monomers and polymer structures.

■ ASSOCIATED CONTENT

Supporting Information

The Supporting Information is available free of charge on the ACS Publications website at DOI: 10.1021/acs.jpcc.8b08984.

Materials, synthesis, and characterization of polymer ligands and quantum dots, including procedures for GPC purification and ligand exchange; centrifugal dialysis filter tests and PL control measurements (Figures S1−S8) (PDF)

■ AUTHOR INFORMATION

Corresponding Author

*E-mail: greytak@sc.edu.

ORCID

Yucheng Huang: 0000-0002-2367-6199

Brian C. Benicewicz: 0000-0003-4130-1232

Andrew B. Greytak: 0000-0001-8978-6457

Present Address

†School of Medicine, University of North Carolina, Chapel Hill, North Carolina 27516, United States (A.F.L.).

Notes

The authors declare no competing financial interest.

■ ACKNOWLEDGMENTS

This work is supported in part by NSF grant number 1613388. A.F.L. acknowledges support from the University of South Carolina, including a Magellan Scholarship and a Science Undergraduate Research Fellowship from the USC Honors College. J.H.D. is additionally supported by an NSF IGERT Graduate Fellowship under grant number 1250052. B.C.B. and Y.H. acknowledge support from the SC SmartState program. We thank Dr. Rui Tan and Stephen K. Roberts for synthesizing core/shell QDs. The authors also thank Dr. Pravin Paudel, Preecha Kittikhunnatham, Megan Y. Gee, and Adam Roberge for helpful discussions.

■ REFERENCES

(1) Medintz, I. L.; Uyeda, H. T.; Goldman, E. R.; Mattoussi, H. Quantum Dot Bioconjugates for Imaging, Labelling and Sensing. *Nat. Mater.* **2005**, *4*, 435−446.

(2) Smith, A. M.; Duan, H.; Rhyner, M. N.; Ruan, G.; Nie, S. A Systematic Examination of Surface Coatings on the Optical and Chemical Properties of Semiconductor Quantum Dots. *Phys. Chem. Chem. Phys.* **2006**, *8*, 3895−3903.

(3) Wu, X.; Liu, H.; Liu, J.; Haley, K. N.; Treadway, J. A.; Larson, J. P.; Ge, N.; Peale, F.; Bruchez, M. P. Immunofluorescent Labeling of Cancer Marker Her2 and Other Cellular Targets with Semiconductor Quantum Dots. *Nat. Biotechnol.* **2003**, *21*, 41−46.

(4) Liu, W.; Choi, H. S.; Zimmer, J. P.; Tanaka, E.; Frangioni, J. V.; Bawendi, M. Compact Cysteine-Coated CdSe(ZnCdS) Quantum

DOI: 10.1021/acs.jpcc.8b08984
J. Phys. Chem. C 2018, 122, 26756−26763

Dots for in Vivo Applications. *J. Am. Chem. Soc.* **2007**, *129*, 14530−14531.
(5) Uyeda, H. T.; Medintz, I. L.; Jaiswal, J. K.; Simon, S. M.; Mattoussi, H. Synthesis of Compact Multidentate Ligands to Prepare Stable Hydrophilic Quantum Dot Fluorophores. *J. Am. Chem. Soc.* **2005**, *127*, 3870−3878.
(6) Liu, W.; Howarth, M.; Greytak, A. B.; Zheng, Y.; Nocera, D. G.; Ting, A. Y.; Bawendi, M. G. Compact Biocompatible Quantum Dots Functionalized for Cellular Imaging. *J. Am. Chem. Soc.* **2008**, *130*, 1274−1284.
(7) Zhu, Z.-J.; Yeh, Y.-C.; Tang, R.; Yan, B.; Tamayo, J.; Vachet, R. W.; Rotello, V. M. Stability of Quantum Dots in Live Cells. *Nat. Chem.* **2011**, *3*, 963−968.
(8) Yildiz, I.; McCaughan, B.; Cruickshank, S. F.; Callan, J. F.; Raymo, F. M. Biocompatible CdSe−ZnS Core−Shell Quantum Dots Coated with Hydrophilic Polythiols. *Langmuir* **2009**, *25*, 7090−7096.
(9) Smith, A. M.; Nie, S. Minimizing the Hydrodynamic Size of Quantum Dots with Multifunctional Multidentate Polymer Ligands. *J. Am. Chem. Soc.* **2008**, *130*, 11278−11279.
(10) Greytak, A. B.; Allen, P. M.; Liu, W.; Zhao, J.; Young, E. R.; Popović, Z.; Walker, B. J.; Nocera, D. G.; Bawendi, M. G. Alternating Layer Addition Approach to CdSe/CdS Core/Shell Quantum Dots with Near-Unity Quantum Yield and High on-Time Fractions. *Chem. Sci.* **2012**, *3*, 2028−2034.
(11) Liu, W.; Greytak, A. B.; Lee, J.; Wong, C. R.; Park, J.; Marshall, L. F.; Jiang, W.; Curtin, P. N.; Ting, A. Y.; Nocera, D. G.; Fukumura, D.; Jain, R. K.; Bawendi, M. G. Compact Biocompatible Quantum Dots via RAFT-Mediated Synthesis of Imidazole-Based Random Copolymer Ligand. *J. Am. Chem. Soc.* **2010**, *132*, 472−483.
(12) Petryayeva, E.; Krull, U. J. Quantum Dot and Gold Nanoparticle Immobilization for Biosensing Applications Using Multidentate Imidazole Surface Ligands. *Langmuir* **2012**, *28*, 13943−13951.
(13) Palui, G.; Aldeek, F.; Wang, W.; Mattoussi, H. Strategies for Interfacing Inorganic Nanocrystals with Biological Systems Based on Polymer-Coating. *Chem. Soc. Rev.* **2015**, *44*, 193−227.
(14) Wang, W.; Kapur, A.; Ji, X.; Safi, M.; Palui, G.; Palomo, V.; Dawson, P. E.; Mattoussi, H. Photoligation of an Amphiphilic Polymer with Mixed Coordination Provides Compact and Reactive Quantum Dots. *J. Am. Chem. Soc.* **2015**, *137*, 5438−5451.
(15) Anderson, N. C.; Chen, P. E.; Buckley, A. K.; De Roo, J.; Owen, J. S. Stereoelectronic Effects on the Binding of Neutral Lewis Bases to CdSe Nanocrystals. *J. Am. Chem. Soc.* **2018**, *140*, 7199−7205.
(16) Popović, Z.; Liu, W.; Chauhan, V. P.; Lee, J.; Wong, C.; Greytak, A. B.; Insin, N.; Nocera, D. G.; Fukumura, D.; Jain, R. K.; et al. A Nanoparticle Size Series for In Vivo Fluorescence Imaging. *Angew. Chem., Int. Ed.* **2010**, *49*, 8649−8652.
(17) Viswanath, A.; Shen, Y.; Green, A. N.; Tan, R.; Greytak, A. B.; Benicewicz, B. C. Copolymerization and Synthesis of Multiply Binding Histamine Ligands for the Robust Functionalization of Quantum Dots. *Macromolecules* **2014**, *47*, 8137−8144.
(18) Johnson, C. M.; Pate, K. M.; Shen, Y.; Viswanath, A.; Tan, R.; Benicewicz, B. C.; Moss, M. A.; Greytak, A. B. A Methacrylate-Based Polymeric Imidazole Ligand Yields Quantum Dots with Low Cytotoxicity and Low Nonspecific Binding. *J. Colloid Interface Sci.* **2015**, *458*, 310−314.
(19) Zhao, X.; Shen, Y.; Adogla, E. A.; Viswanath, A.; Tan, R.; Benicewicz, B. C.; Greytak, A. B.; Lin, Y.; Wang, Q. Surface Labeling of Enveloped Virus with Polymeric Imidazole Ligand-Capped Quantum Dots via the Metabolic Incorporation of Phospholipids Into Host Cells. *J. Mater. Chem. B* **2016**, *4*, 2421−2427.
(20) Lin, C.-A. J.; Sperling, R. A.; Li, J. K.; Yang, T.-Y.; Li, P.-Y.; Zanella, M.; Chang, W. H.; Parak, W. J. Design of an Amphiphilic Polymer for Nanoparticle Coating and Functionalization. *Small* **2008**, *4*, 334−341.
(21) Wang, W.; Ji, X.; Na, H. B.; Safi, M.; Smith, A.; Palui, G.; Perez, J. M.; Mattoussi, H. Design of a Multi-Dopamine-Modified Polymer Ligand Optimally Suited for Interfacing Magnetic Nanoparticles with Biological Systems. *Langmuir* **2014**, *30*, 6197−6208.
(22) Zhang, P.; Liu, S.; Gao, D.; Hu, D.; Gong, P.; Sheng, Z.; Deng, J.; Ma, Y.; Cai, L. Click-Functionalized Compact Quantum Dots Protected by Multidentate-Imidazole Ligands: Conjugation-Ready Nanotags for Living-Virus Labeling and Imaging. *J. Am. Chem. Soc.* **2012**, *134*, 8388−8391.
(23) Wang, W.; Ji, X.; Kapur, A.; Zhang, C.; Mattoussi, H. A Multifunctional Polymer Combining the Imidazole and Zwitterion Motifs as a Biocompatible Compact Coating for Quantum Dots. *J. Am. Chem. Soc.* **2015**, *137*, 14158−14172.
(24) Wang, W.; Kapur, A.; Ji, X.; Zeng, B.; Mishra, D.; Mattoussi, H. Multifunctional and High Affinity Polymer Ligand That Provides Bio-Orthogonal Coating of Quantum Dots. *Bioconjugate Chem.* **2016**, *27*, 2024−2036.
(25) Chiefari, J.; Chong, Y. K.; Ercole, F.; Krstina, J.; Jeffery, J.; Le, T. P. T.; Mayadunne, R. T. A.; Meijs, G. F.; Moad, C. L.; Moad, G.; et al. Living Free-Radical Polymerization by Reversible Addition−Fragmentation Chain Transfer: The RAFT Process. *Macromolecules* **1998**, *31*, 5559−5562.
(26) Tasso, M.; Giovanelli, E.; Zala, D.; Bouccara, S.; Fragola, A.; Hanafi, M.; Lenkei, Z.; Pons, T.; Lequeux, N. Sulfobetaine-Vinylimidazole Block Copolymers: A Robust Quantum Dot Surface Chemistry Expanding Bioimaging's Horizons. *ACS Nano* **2015**, *9*, 11479−11489.
(27) Trapiella-Alfonso, L.; Pons, T.; Lequeux, N.; Leleu, L.; Grimaldi, J.; Tasso, M.; Oujagir, E.; Seguin, J.; d'Orlye, F.; Girard, C.; et al. Clickable-Zwitterionic Copolymer Capped-Quantum Dots for in Vivo Fluorescence Tumor Imaging. *ACS Appl. Mater. Interfaces* **2018**, *10*, 17107−17116.
(28) Viswanath, A.; Paudel, P.; Kittikhunnatham, P.; Green, A. N.; Greytak, A. B.; Benicewicz, B. C. Synthesis of Random Terpolymers Bearing Multidentate Imidazole Units and Their Use in Functionalization of Cadmium Sulfide Nanowires. *Polym. Chem.* **2015**, *6*, 7036−7044.
(29) Shen, Y.; Gee, M. Y.; Tan, R.; Pellechia, P. J.; Greytak, A. B. Purification of Quantum Dots by Gel Permeation Chromatography and the Effect of Excess Ligands on Shell Growth and Ligand Exchange. *Chem. Mater.* **2013**, *25*, 2838−2848.
(30) Shen, Y.; Roberge, A.; Tan, R.; Gee, M. Y.; Gary, D. C.; Huang, Y.; Blom, D. A.; Benicewicz, B. C.; Cossairt, B. M.; Greytak, A. B. Gel Permeation Chromatography as a Multifunctional Processor for Nanocrystal Purification and On-Column Ligand Exchange Chemistry. *Chem. Sci.* **2016**, *7*, 5671−5679.
(31) Shen, Y.; Tan, R.; Gee, M. Y.; Greytak, A. B. Quantum Yield Regeneration: Influence of Neutral Ligand Binding on Photophysical Properties in Colloidal Core/Shell Quantum Dots. *ACS Nano* **2015**, *9*, 3345−3359.
(32) Anderson, N. C.; Hendricks, M. P.; Choi, J. J.; Owen, J. S. Ligand Exchange and the Stoichiometry of Metal Chalcogenide Nanocrystals: Spectroscopic Observation of Facile Metal-Carboxylate Displacement and Binding. *J. Am. Chem. Soc.* **2013**, *135*, 18536−18548.

DOI: 10.1021/acs.jpcc.8b08984
J. Phys. Chem. C 2018, 122, 26756−26763